

A theoretical study on chemical ordering of 38-atom trimetallic Pd-Ag-Pt nanoalloys

Songül Taran, Ali Kemal Garip, Haydar Arslan

Citation: Chin. Phys. B . 2020, 29(7): 077801 . **doi:** 10.1088/1674-1056/ab99b4
Journal homepage: http://cpb.iphy.ac.cn; http://iopscience.iop.org/cpb

What follows is a list of articles you may be interested in

Cascaded plasmonic nanorod antenna for large broadband local electric field enhancement

Dou Zhang(张豆), Zhong-Jian Yang(杨中见), Jun He(何军)

Chin. Phys. B . 2019, 28(10): 107802 . **doi:** 10.1088/1674-1056/ab3f99

Hot spots enriched plasmonic nanostructure-induced random lasing of quantum dots thin film

Feng Shan(单锋), Xiao-Yang Zhang(张晓阳), Jing-Yuan Wu(吴静远), Tong Zhang(张彤)

Chin. Phys. B . 2018, 27(4): 047804 . **doi:** 10.1088/1674-1056/27/4/047804

Effects of (La, Sr) co-doping on electrical conduction and magnetic properties of $BiFeO_3$ nanoparticles

Li Liu(刘莉), Shouyu Wang(王守宇), Zi Yin(殷子), Weifang Liu(刘卫芳), Xunling Xu(徐训岭), Chuang Zhang(张闯), Xiu Li(李秀), Jiabin Yang(杨佳斌)

Chin. Phys. B . 2016, 25(9): 097801 . **doi:** 10.1088/1674-1056/25/9/097801

Spectral features and antibacterial properties of Cu-doped ZnO nanoparticles prepared by sol-gel method

Alireza Samavati, A F Ismail, Hadi Nur, Z Othaman, M K Mustafa

Chin. Phys. B . 2016, 25(7): 077803 . **doi:** 10.1088/1674-1056/25/7/077803

Second harmonic generation of metal nanoparticles under tightly focused illumination

Jing-Wei Sun(孙经纬), Xiang-Hui Wang(王湘晖), Sheng-Jiang Chang(常胜江),Ming Zeng(曾明), Na Zhang(张娜)

Chin. Phys. B . 2016, 25(3): 037803 . **doi:** 10.1088/1674-1056/25/3/037803

A theoretical study on chemical ordering of 38-atom trimetallic Pd–Ag–Pt nanoalloys

Songül Taran[1,†], Ali Kemal Garip[2], and Haydar Arslan[2]

[1] *Department of Physics, Duzce University, Duzce* 81620, *Turkey*
[2] *Department of Physics, Zonguldak Bulent Ecevit University, Zonguldak* 67100, *Turkey*

(Received 25 March 2020; revised manuscript received 28 May 2020; accepted manuscript online 5 June 2020)

In this study, truncated octahedron (TO) structure is selected for further analysis and we focus on 38-atom Pd–Pt–Ag trimetallic nanoalloys. The best chemical ordering structures of $Pd_nAg_{32-n}Pt_6$ trimetallic nanoalloys are obtained at Gupta level. The structures with the lowest energy at Gupta level are then re-optimized by density functional theory (DFT) relaxations and DFT results confirm the Gupta level calculations with small shifts on bond lengths indicating TO structure is favorable for 38-atom of $Pd_nAg_{32-n}Pt_6$ trimetallic nanoalloys. The DFT excess energy analysis shows that $Pd_8Ag_{24}Pt_6$ composition has the lowest excess energy value in common with excess energy analysis at Gupta level. In $Pd_8Ag_{24}Pt_6$ composition, eight Pd atoms are central sites of 8 (111) hexagonal facets of TO, 24 Ag atoms locate on surface, and 6 Pt atoms locate at the core of the structure. It is also obtained that all of the compositions except $Pd_{18}Ag_{14}Pt_6$ and $Pd_{20}Ag_{12}Pt_6$ exhibit a octahedral Pt core. Besides, it is observed that there is a clear tendency for Ag atoms to segregate to the surface and also Pt atoms prefer to locate at core due to order parameter (R) variations.

Keywords: nanoalloys, chemical ordering, optimization, density functional theory (DFT)

PACS: 78.67.Bf, 31.15.E–, 36.40.–c **DOI:** 10.1088/1674-1056/ab99b4

1. Introduction

Recently, the focus of clusters has been shifting toward nanoalloys consisting of two or more different metals within nanometer size.[1] The size-dependent tunability of nanoalloys offers an excellent opportunity for tailoring new nanoscale materials.[2] Besides, nanoalloys offer the opportunity for tailoring the structures and properties of materials through the choice of atom type and composition.[3,4] Alloying of two or more metals at nanosize is of interest especially for catalysts since the combination of metals can increase the activity and/or the selectivity of catalysts.[5] Since the activity and selectivity are closely associated with structure, their surface structures, compositions, and segregation properties are of particular interest.[6] One promising route to determine and increase the catalytic performance is properly controlling of the size, structure, and composition of nanoalloys.[7] In addition to the geometry and size of the particles, catalytic performance of nanoalloys depends on the chemical ordering.[8] For this reason, a theoretical study of nanoalloys is important in order to find and develop the properties which they attain when their geometric structure and chemical composition varies.[2]

The reason for concentrating here on truncated octahedron (TO) structure is that the selected motif possesses high symmetry,[9] and frequently adopted in theoretical and experimental studies.[10] The 38-atom TO was chosen as model for the trimetallic nanoalloys due to the high symmetry of the parent TO structure (O_h)[11] with 8 (111) hexagonal and 6 (100) square faces.[12] Besides, the size is interesting since it corresponds to magic number of atoms for the truncated octahedron[13] and it is the only size below 50 atoms at which fcc structures are in competition with icosahedral fragments and amorphous structures.[14] Furthermore, it was found that TO structures typically dominate 38-atom nanoclusters in several studies of literature and also they were obtained as the global minimum (GM) for many clusters for the Gupta many body potential,[4,15,16] as well as the other many-body and pair potentials.[17–19]

There have been many theoretical studies of mono and bimetallic nanoclusters with 38-atom TO structure to investigate the relationship between geometric structure, chemical ordering and segregation tendency.[2,4–11,14,15,20–25] Zhu *et al.*[7] investigated Pd–Au nanoalloys for 38-atom TO. Demiroğlu *et al.*[11] performed a density functional theory (DFT) study to investigate the effect of the TiO_2 support on the structures of 38-atom AuRh nanoalloys and in another study nanoscale mixing properties of 38-atom Au–Rh were investigated.[8] Roy *et al.*[20] studied 38-atom Pd–Pt, Ag–Au, Pd–Au, and Ag–Pt binary clusters combining empirical potential (EP) and DFT calculations. Rodrigues *et al.*[2] calculated the global optimization of Cu_nAu_m ($n+m=38$) clusters. A study of chemical ordering in 38-atom Pd–Ir nanoalloys were reported by Davis *et al.*[5] Cerbelaud *et al.*[21] determined the optimal chemical ordering for binary AgAu cluster with 38-atom. Curley *et al.*[6] studied the Ag–Au bimetallic nanoalloy clusters with 38 atoms using Gupta many-body potential. For chemical ordering in AgAu TO nanoalloys of

†Corresponding author. E-mail: songultaran@duzce.edu.tr

© 2020 Chinese Physical Society and IOP Publishing Ltd

38 atoms, Rapetti *et al.*[14] also reported a DFT global optimization study. Darby *et al.*[4] reported that Cu_{38} and Au_{38} clusters have a TO structure. Molayem *et al.*[22] found global minimum structures based on TO for some Cu–Ag nanoalloys with 38 atoms. A theoretical investigation of 38-atom CuPt clusters was performed by Guerrero-Jordan *et al.*[23] using a genetic algorithm. Pittaway *et al.*[24] also used genetic algorithm for global optimization of 38-atom PdAu clusters with TO structure. Fan *et al.*[10] investigated the structural stability and chemical ordering of 38-atom TO Pd–Ir nanoalloys. Melting mechanism of $Pd_{24}Pt_{14}$ nanoalloy with TO was determined by Oderji *et al.*[25] Negreiros *et al.*[9] analyzed the kinetics of chemical ordering in a Ag–Pt TO nanoalloy particle via first principles simulations. TO structure and energetics of Ni, Ag, and Au nanoclusters of size 38 atoms were investigated by Michaelian *et al.*[15]

Despite of these investigations on the monometallic and bimetallic nanoclusters with 38-atom TO structure, there are not sufficient data about trimetallic 38-atom nanoclusters. Pacheco-Contreras *et al.*[13] investigated Ag–Au–Pt trimetallic clusters contain a total of 38 atoms at Gupta and DFT levels. Wu *et al.*[26] investigated geometrical and energetic properties in 38-atom Au–Pd–Pt clusters. The structrures of $Cu_8Au_nPt_{30-n}$ clusters were analyzed by Wu *et al.*[27] Besides, many above-mentioned investigations performed simulation searches by combining EP and DFT approaches. Since there is still lacking a thorough study presenting the relationship between geometric structure, chemical ordering, and segregation tendency of trimetallic nanoalloys with 38-atom TO, we have focused on 38-atom Pd–Pt–Ag trimetallic nanoalloys with TO structure in this study. Although some investigations[28,29] on clusters present comparisons with available experimental results, it is not always possible to directly compare theoretical results with experimental data for clusters. To study small clusters with rather accurate methods from the theoretical point of view, DFT calculations could be an alternative choice. Thus, we have performed DFT re-optimization for the best chemical ordering structures of $Pd_nAg_{32-n}Pt_6$ trimetallic nanoalloys obtained at Gupta level.

2. Computational methods

In order to model the metallic bonding between Pt, Pd, and Ag atoms in Pd–Ag–Pt trimetallic naoalloys, Gupta potential[30,31] has been used. Gupta potential can be written in terms of repulsive (V_i^{r}) and attractive (V_i^{m}) many-body terms and the functional form is given by

$$V = \sum_{i}^{N} (V_i^{\mathrm{r}} - V_i^{\mathrm{m}}), \tag{1}$$

$$V_i^{\mathrm{r}} = \sum_{j\neq i}^{N} A(a,b) \exp\left[-p(a,b)\left(\frac{r_{ij}-r_0(a,b)}{r_0(a,b)}\right)\right], \tag{2}$$

$$V_i^{\mathrm{m}} = \left\{\sum_{j\neq i}^{N} \xi^2(a,b) \exp\left[-2q(a,b)\left(\frac{r_{ij}-r_0(a,b)}{r_0(a,b)}\right)\right]\right\}^{1/2}, \tag{3}$$

where A, r_0, ξ, p, and q are adjustable parameters.[32] The numerical values of the above Gupta parameters are listed in Table 1. The Gupta potential parameters used in this study are taken from Ref. [33].

Table 1. The Gupta potential parameters for Pt–Pd–Ag trimetallic clusters.

	A/eV	ζ/eV	p	q	r_0/Å
Pd–Pd	0.1746	1.7180	10.867	3.742	2.7485
Pd–Pt	0.2300	2.2000	10.740	3.870	2.7600
Pd–Ag	0.1610	1.5597	10.895	3.492	2.8200
Pt–Pt	0.2975	2.6950	10.612	4.004	2.7747
Pt–Ag	0.1750	1.7900	10.730	3.570	2.8330
Ag–Ag	0.1031	1.1895	10.850	3.180	2.8921

The best chemical ordering structures of $Pd_nAg_{(32-n)}Pt_6$ nanoalloys with TO structure were carried out using Monte Carlo Basin–Hopping algorithm.[34,35] The best chemical ordering structures obtained at Gupta level were chosen as initial configurations and re-optimized DFT searches were performed for the chemical ordering in $Pd_nAg_{(32-n)}Pt_6$ nanoalloys. The DFT calculations with Perdew–Burke–Ernzerhof (PBE) exchange–correlation functional[36] were made by using the Quantum ESPRESSO package.[37,38] In Quantum ESPRESSO, the energy cutoff for wavefunctions was used as 45.0 Ry (1 Ry = 13.6056923(12) eV) and the cutoff energy for charge density was used as 448.0 Ry.

3. Results and discussion

In the current study, chemical ordering in 38-atom trimetallic Pd–Ag–Pt nanoalloys with TO structure has been studied and a systematic search was performed for the best chemical ordering structures. Besides, structure and chemical ordering effect on stability of trimetallic nanoalloys are explored. Structural details of trimetallic nanoalloys are analyzed as a function of their chemical compositions. We mainly focus here on the $Pd_nAg_{(32-n)}Pt_6$ nanoalloys with fixed six Pt atoms where the fixed number 6 represents inner atoms of the 38-atom TO structure. The high-symmetry structure is taken as initial atomic configurations.

The best chemical ordering structures obtained at Gupta level for $Pd_nAg_{(32-n)}Pt_6$ nanoalloys are presented in Fig. 1. As can be seen from the figure our simulations did not break the initial symmetry and in general, Pt atoms are preferentially placed in the inner part of the nanoalloys. In $Pd_{18}Ag_{14}Pt_6$ and $Pd_{20}Ag_{12}Pt_6$ compositions one Pd atom locates at core with 5 Pt atoms by replacing one Pt atom. Since the number of Pt atoms is constant to 6, the compositions except $Pd_{18}Ag_{14}Pt_6$ and $Pd_{20}Ag_{12}Pt_6$ exhibit a octahedral Pt core. For $Ag_{32}Pt_6$

bimetallic nanalloy, Ag atoms tend to segregate to the surface and Pt atoms tend to segregate into the structure core. In $Pd_nAg_{(32-n)}Pt_6$ trimetallic nanoalloys, with the increase of Pd atoms from 1 to 8, the Pd atoms locate at the center of hexagonal facets of TO. It is well known that 38-atom TO structure has 8 (111) hexagonal and each (111) facets has 7 atoms composed of 6 sites on the vertexes of hexagon and 1 central site. Besides, 38-atom TO structure has six (100) square facets and each (100) facets has 4 atoms. At $n_{Pd} = 9$–14, each of the added six Pd atoms locates on one of the six (100) facets. With the further increase of Pd atoms, the locating tendency of Pd atoms can be identified as growing on the sites on the adjoining edges of (100) and (111) facets.

In the nanoscale, the energetic stability among a family of nanoalloys is determined by calculating the excess energy (ΔE_{exc}). For trimetallic $Pd_nAg_{(32-n)}Pt_6$ nanoalloys with fixed size but different compositions excess energy is defined as[39]

$$\Delta E_{exc}^{Gupta} = E(Pd_n\,Ag_{32-n}\,Pt_6) - n\frac{E(Pd_{32}\,Pt_6)}{32} - (32-n)\frac{E(Ag_{32}\,Pt_6)}{32}, \quad (4)$$

where $E(Pd_n\,Ag_{32-n}\,Pt_6)$ is the Gupta total energy of the trimetallic nanoalloys and $E(Pd_{32}\,Pt_6)$ and $E(Ag_{32}\,Pt_6)$ are the total energies of the binary Pd–Pt and Ag–Pt bimetallic nanoalloys. This equation is also used for ΔE_{exc}^{DFT} where $E(Pd_n\,Ag_{32-n}\,Pt_6)$, $E(Pd_{32}\,Pt_6)$, and $E(Ag_{32}\,Pt_6)$ are the DFT total energies.

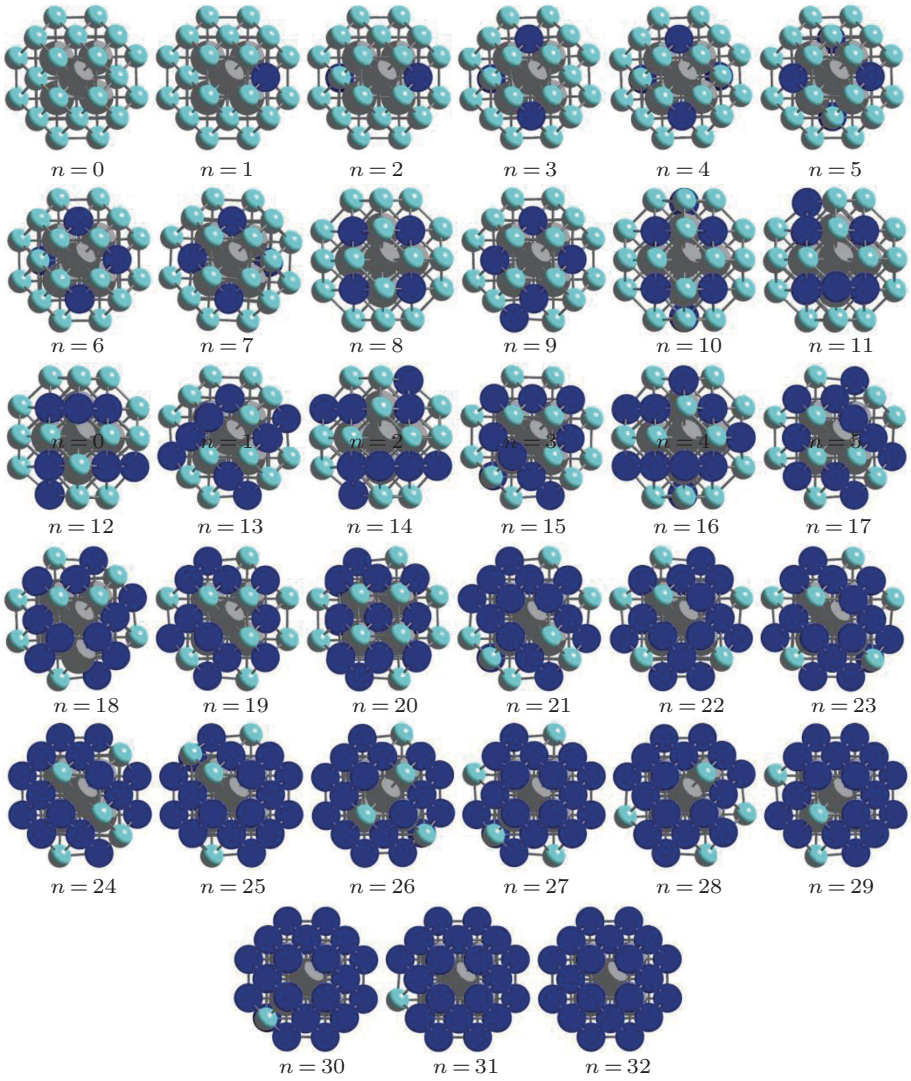


Fig. 1. The best chemical ordering structures of 38-atom trimetallic $Pd_nAg_{32-n}Pt_6$ nanoclusters. The dark blue, light blue, and grey colors represent Pd, Ag, and Pt atoms, respectively.

In order to provide more useful structural information about the chosen nanoalloy system, Gupta and DFT approaches were combined. The best chemical ordering structures at Gupta level were recalculated with DFT relaxations to crosscheck the lowest energy structures. Since there is not occurrence of any discrepancies on nanoalloy structures, it can be interpreted as DFT results confirm the Gupta level calculations with small shifts on bond lengths. Also, DFT calculations indicate that the truncated octahedron structure is indeed the lowest energy ones for $Pd_nAg_{(32-n)}Pt_6$ nanoalloys. Fig-

ure 2 shows the plots of excess energy as a function of composition for 38-atom nanoalloys at Gupta and DFT levels. It is worth mentioning that the lowest excess energy values were obtained at the same composition of $Pd_8Ag_{24}Pt_6$ at Gupta and DFT levels since Gupta and DFT excess energy variations exhibit quite compatible behaviors. In $Pd_8Ag_{24}Pt_6$ composition, 8 Pd atoms are central sites of 8 (111) hexagonal facets of TO, 24 Ag atoms locate on surface, and 6 Pt atoms locate at the core of the structure.

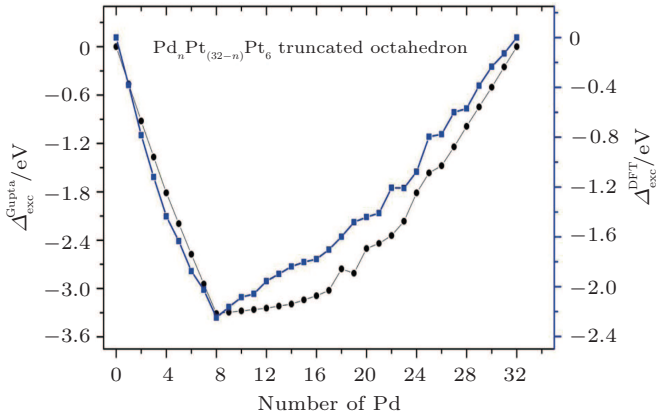


Fig. 2. Excess energy of 38-atom trimetallic $Pd_nAg_{32-n}Pt_6$ nanoclusters at Gupta and DFT levels.

The structure of the most stable composition $Pd_8Ag_{24}Pt_6$ for $Pd_nAg_{32-n}Pt_6$ nanoalloys is illustrated in detail in Fig. 3. It is clear from the figure that, Pd, Ag, and Pt atoms of the $Pd_8Ag_{24}Pt_6$ composition are located more symmetrically. Figure 4 shows the two different chemical orderings of $Pd_{18}Ag_{14}Pt_6$ and $Pd_{20}Ag_{12}Pt_6$ nanoalloy structures at DFT level. Since one Pd atom locates at core with 5 Pt atoms for these two compositions, we researched what would be their energies if the surface Pt atom is in the core. The top row represents the re-optimization structures obtained at Gupta level and the bottom row represents the structures with Pt atoms forming core for $Pd_{18}Ag_{14}Pt_6$ and $Pd_{20}Ag_{12}Pt_6$ nanoalloys in Figs. 4(a) and 4(b), respectively. For $Pd_{18}Ag_{14}Pt_6$ composition, the DFT analysis shows that the structure obtained at Gupta level is 0.026-eV higher in energy than the structure which has 6 Pt atoms in its core. However, the DFT analysis is also found in close competition for $Pd_{20}Ag_{12}Pt_6$ as the re-optimization structure obtained at Gupta level is only 0.001-eV higher in energy. According to these results, it seems that the chemical orderings which correspond to Gupta level minima are energetically favorable for both $Pd_{18}Ag_{14}Pt_6$ and $Pd_{20}Ag_{12}Pt_6$ nanoalloys.

In order to better discuss about the atomic mixing degree of different type atoms in Pd–Ag–Pt nanoalloys, the order parameter (R_A)[40] is adopted. R_A can be defined by the average distance of a type of atoms from the center of a cluster, *i.e.*,

$$R_A = \frac{1}{n_A}\sum_{i=1}^{n_A}\sqrt{x_i^2+y_i^2+z_i^2}, \tag{5}$$

where n_A is the A atom number in the trimetallic nanoalloys, and x_i, y_i, and z_i show the positions of the atoms. Large and small R_A values point out that the atoms are at surface and center, respectively with a segregated pattern and also, the medium values implies a well-mixed nanoalloy.

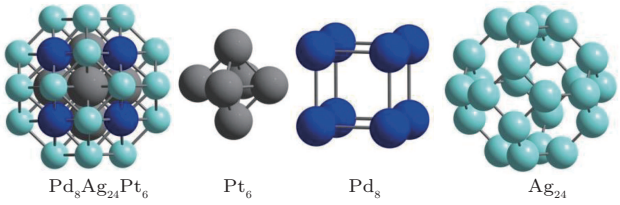


Fig. 3. The location of Pt, Pd, and Ag atoms of the most stable $Pd_8Ag_{24}Pt_6$ composition for $Pd_nAg_{32-n}Pt_6$.

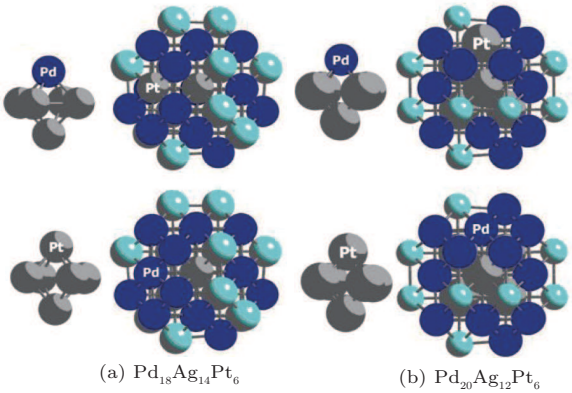


Fig. 4. Two different chemical orderings of (a) $Pd_{18}Ag_{14}Pt_6$ and (b) $Pd_{20}Ag_{12}Pt_6$ nanoalloy structures at DFT level. The top row represents the re-optimization structures obtained at Gupta level and the bottom row represents the structures with Pt atoms forming core.

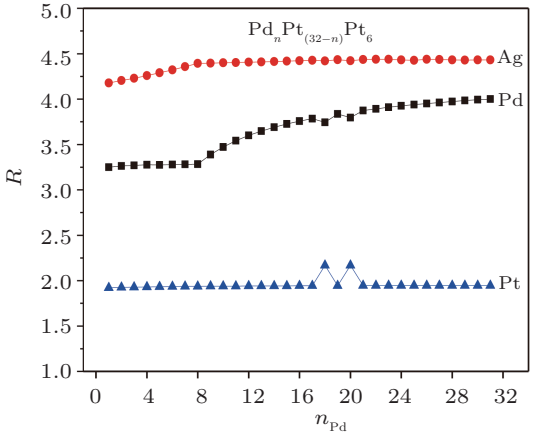


Fig. 5. The order parameter (R) variation of trimetallic $Pd_nAg_{32-n}Pt_6$ nanoalloys.

Figure 5 shows the order parameter (R) variation of trimetallic $Pd_nAg_{32-n}Pt_6$ nanoalloys. As can be seen from the figure R_{Ag} value is larger than R_{Pd} and R_{Pd} is larger than R_{Pt} for most of the compositions. It indicates that there is a clear tendency for Ag atoms to segregate to the surface of the nanoalloys and also Pt atoms prefer to locate at core. For $n_{Pd} = 1$–8, R_{Pd} parameter values keep constant as 8 Pd atoms occupy the central sites of 8 (111) hexagonal facets. In the size range of $n_{Pd} = 9$–31, R_{Pd} parameter values gradually increase with

the increasing concentration of surface Pd atoms. The change reason of the R_{Pt} parameter at $n_{Pd} = 18$ and 20 is that the replacement of one Pt atom in the core with one Pd atom on the surface.

The strain effects are more important in the bimetallic and trimetallic systems, because of the size mismatch between different atomic species. Also, the strain becomes different in different geometries, indicating that the chosen geometry and chemical ordering are interrelated. Since nanoparticles with strained surfaces may present important catalytic properties, we decided to investigate the local atomic pressure values for Pd–Ag–Pt nanoalloys. The local pressure P_i acting on atom i is proportional to the trace of the tensor given as follows:[41,42]

$$P_i = -\frac{1}{3}\mathrm{Tr}(\sigma_i), \tag{6}$$

where σ_i is atomic stress tensor. P_i can assume positive and negative values. $P_i > 0$ indicates compressive stress on atom i and $P_i < 0$ indicates tensile stress on atom i. If $P_i = 0$, it indicates the absence of stress.[42]

Figure 6 shows the local atomic pressures for $Ag_{32}Pt_6$, $Pd_{32}Pt_6$, and $Pd_8Ag_{24}Pt_6$ nanoalloys to compare the most stable structure of trimetallic ($Pd_8Ag_{24}Pt_6$) and bimetallic ($Ag_{32}Pt_6$, $Pd_{32}Pt_6$) nanoalloys. For $Ag_{32}Pt_6$ bimetallic nanoalloy, 6 Pt atoms locate at the core and their pressure values are strongly positive. The 32 Ag atoms locate on the surface due to lower surface energy. The 8 Ag atoms on surface are central sites of 8 (111) hexagonal facets and they present positive pressure value as remaining Pd atoms present negative local atomic pressure. The pressure on the surface is in the range between −4 GPa and 3 GPa for $Ag_{32}Pt_6$ bimetallic nanoalloy. As for $Pd_{32}Pt_6$ bimetallic nanoalloy, Pd atoms fully occupy the surface and 6 Pt atoms occupy the core of the structure. The pressure of the inner Pt atoms is also strongly positive. The 8 Pd atoms at central sites of 8 (111) hexagonal facets have positive pressure values and pressure becomes negative for remaining 24 Pd atoms. The pressure on the surface is in the range between −6 GPa and 2 GPa for $Pd_{32}Pt_6$ bimetallic nanoalloy. $Pd_8Ag_{24}Pt_6$ trimetallic nanoalloy is also has a core composed of 6 Pt atoms which have strongly positive pressure values, similar to these two bimetallic compositions. The 8 Pd atoms especially locate at central sites of 8 (111) hexagonal facets and the pressure at the central sites becomes more positive than bimetallic ones indicating the strain is more compressive. For $Pd_8Ag_{24}Pt_6$ nanoalloy, the pressure on the surface is in the range between −5 GPa and 4 GPa. The 24 Ag atoms locate on the adjoining edges of (100) and (111) facets and they exhibit negative pressure. As can be seen from the pressure scale, it can be interpreted as that the substituted atoms on surface present mildly pressure range for trimetallic nanoalloy.

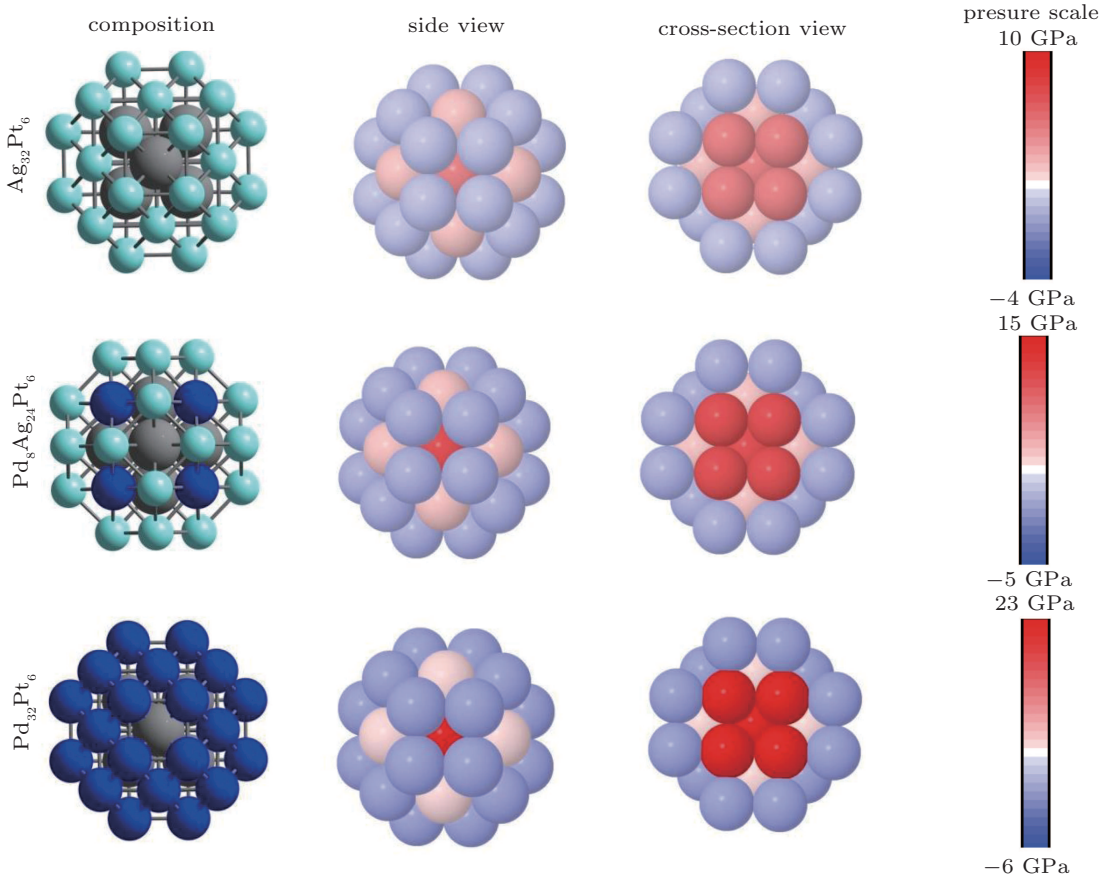


Fig. 6. Local atomic pressure for $Ag_{32}Pt_6$, $Pd_{32}Pt_6$, and $Pd_8Ag_{24}Pt_6$ nanoalloys.

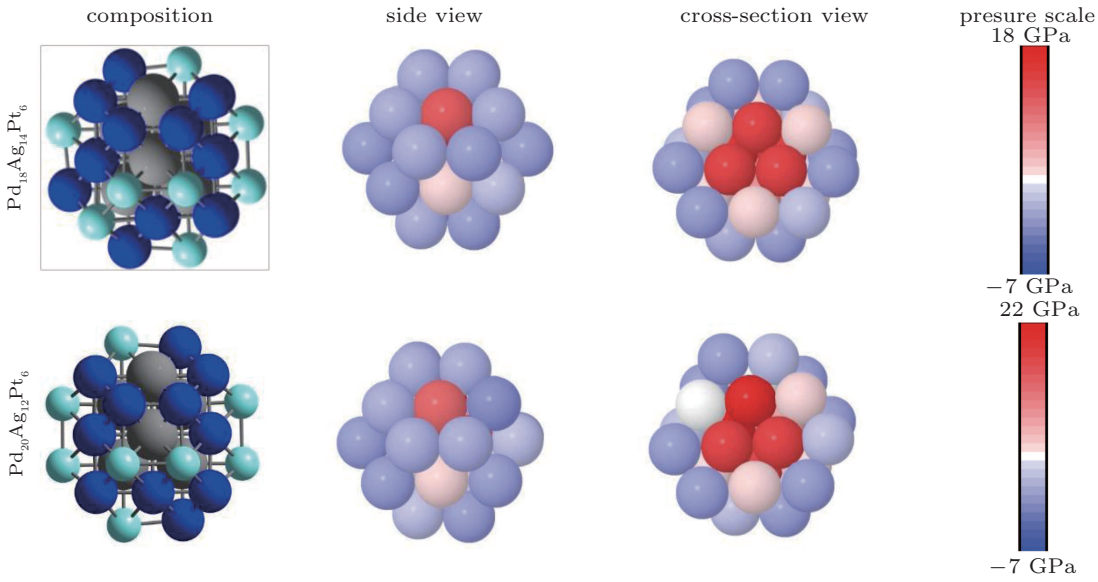


Fig. 7. The local atomic pressure for $Pd_{18}Ag_{14}Pt_6$ and $Pd_{20}Ag_{12}Pt_6$ nanoalloys.

Figure 7 shows the local atomic pressure for $Pd_{18}Ag_{14}Pt_6$ and $Pd_{20}Ag_{12}Pt_6$ nanoalloys. As can be seen from the side views of these two nanoalloys, one Pt atom locates on central site of (111) hexagonal facet and presents highly positive pressure which is close to each other. For $Pd_{18}Ag_{14}Pt_6$ nanoalloy, Pd core atom has pressure value about 8 GPa which is the lowest positive pressure in the core. The pressure value of surface Pd atoms exhibits in the range between −5 GPa and 1 GPa. Also, Ag atoms exhibit negative pressure about −7 GPa. For $Pd_{20}Ag_{12}Pt_6$ nanoalloy, Pd core atom has pressure value about 6 GPa which is the lowest positive pressure in the core. The pressure value of surface Pd atoms exhibits in the range between −5 GPa and 0 GPa. Also, Ag atoms exhibit negative pressure about −7 GPa similar to $Pd_{18}Ag_{14}Pt_6$ nanoalloy. According to pressure results of these two compositions, the location of one Pd atom at core with 5 Pt atoms can be attributed to the relaxation of strained core structure.

4. Conclusions

In this study, we have performed a systematic investigation of $Pd_nAg_{32-n}Pt_6$ trimetallic nanoalloys and we have focused on 38-atom Pd–Pt–Ag trimetallic nanoalloys with truncated octahedron (TO) structure. The best chemical ordering structures were obtained using Monte Carlo basin-hopping algorithm within Gupta potential. The structures with the lowest energy at Gupta level are then re-optimized by DFT relaxations and DFT results confirm the Gupta level calculations with small shifts on bond lengths, indicating TO structure is favorable for 38-atom of $Pd_nAg_{32-n}Pt_6$ trimetallic nanoalloys.

In $Pd_nAg_{(32-n)}Pt_6$ trimetallic nanoalloys, all the compositions except $Pd_{18}Ag_{14}Pt_6$ and $Pd_{20}Ag_{12}Pt_6$ nanoalloys exhibit a octahedral Pt core. From the order parameter variations of trimetallic $Pd_nAg_{32-n}Pt_6$ nanoalloys, it was observed that Ag atoms exhibit a clear tendency to segregate to the surface. DFT level investigations showed that two chemical orderings corresponding Gupta level minima with 5 Pt atoms at core (for $Pd_{18}Ag_{14}Pt_6$ and $Pd_{20}Ag_{12}Pt_6$) are energetically favorable than the chemical orderings with 6 Pt atoms at core. Moreover, DFT and Gupta excess energy analysis show that $Pd_8Ag_{24}Pt_6$ composition has the lowest excess energy value which corresponds to more stable structure. In $Pd_8Ag_{24}Pt_6$ composition, 8 Pd atoms are central sites of 8 (111) hexagonal facets of TO, 24 Ag atoms locate on surface and 6 Pt atoms locate at the core of the structure. Furthermore, it was observed that 8 Pd atoms at central sites of hexagonal facets exhibit more positive pressure than the atoms at central sites of bimetallic $Ag_{32}Pt_6$ and $Pd_{32}Pt_6$ nanoalloys in relation to mismatch between three different atomic species and also chemical ordering.

Acknowledgments

The DFT calculations reported in this paper were fully performed at TUBITAK ULAKBIM, High Performance and Grid Computing Center (TRUBA resources).

References

[1] Kaiser J, Leppert L, Welz H, Polzer F, Wunder S, Wanderka N, Albrecht M, Lunkenbein T, Breu J, Kümmel S, Lu Y and Ballauff M 2012 *Phys. Chem. Chem. Phys.* **14** 6487

[2] Rodrigues D D C, Nascimento A M, Duarte H A and Belchior J C 2008 *Chem. Phys.* **349** 91

[3] Chen F and Johnston R L 2008 *ACS Nano* **2** 165

[4] Darby S, Mortimer-Jones T V, Johnston R L and Roberts C 2002 *J. Chem. Phys.* **116** 1536

[5] Davis J B A, Johnston R L, Rubinovich L and Polak M 2014 *J. Chem. Phys.* **141** 224307

[6] Curley B C, Rossi G, Ferrando R and Johnston R L 2007 *Eur. Phys. J. D* **43** 53

[7] Zhu B, Front A, Guesmi H, Creuze J, Legrand B and Mottet C 2017 *Comput. Theor. Chem.* **1107** 49
[8] Demiroglu I, Li Z Y, Piccolo L and Johnston R L 2016 *Catal. Sci. Technol.* **6** 6916
[9] Negreiros F R, Taherkhani F, Parsafar G, Caro A and Fortunelli A 2012 *J. Chem. Phys.* **137** 194302
[10] Fan T E, Demiroglu I, Hussein H A, Liu T D and Johnston R L 2017 *Phys. Chem. Chem. Phys.* **19** 27090
[11] Demiroglu I, Li Z Y, Piccolo L and Johnston R L 2017 *Comput. Theor. Chem.* **1107** 142
[12] Ismail R 2012 *Theoretical studies of free and supported nanoalloy clusters*, Ph. D. Dissertation (The Universiry of Birmingham)
[13] Pacheco-Contreras R, Juárez-Sáchez J O, Dessens-Félix M, Aguilera-Granja F, Fortunelli A and Posada-Amarillas A 2018 *Comput. Mater. Sci.* **141** 30
[14] Rapetti D and Ferrando R 2019 *J. Alloys Compd.* **779** 582
[15] Michaelian K, Rendón N and Garzón I L 1999 *Phys. Rev. B* **60** 2000
[16] Bailey M S, Wilson N T, Roberts C and Johnston R L 2003 *Eur. Phys. J. D* **25** 41
[17] Roberts C, Johnston R L and T W N 2000 *Theor. Chem. Acc.* **104** 123
[18] Doye J P K and Wales D J 1998 *New J. Chem.* **22** 733
[19] Lathiotakis N N, Andriotis A N, Menon M and Connolly J 1996 *J. Chem. Phys.* **104** 992
[20] Johnston R L, Paz-Borbón L O, Barcaro G and Fortunelli A 2008 *J. Chem. Phys.* **128** 134517
[21] Cerbelaud M, Ferrando R, Barcaro G and Fortunelli A 2011 *Phys. Chem. Chem. Phys.* **13** 10232
[22] Molayem M, Grigoryan V G and Springborg M 2011 *J. Phys. Chem. C* **115** 22148
[23] Guerrero-Jordan J, Cabellos J L, Johnston R L and Posada-Amarillas A 2018 *Eur. Phys. J. B* **91** 123
[24] Pittaway F, Paz-Borbón L O, Johnston R L, Arslan H, Ferrando R, Mottet C, Barcaro G and Fortunelli A 2009 *J. Phys. Chem. C* **113** 9141
[25] Oderji H Y and Ding H 2011 *Chem. Phys.* **388** 23
[26] Wu G H, Liu Q M and Wu X 2015 *Chem. Phys. Lett.* **620** 92
[27] Wu G, Sun Y, Wu X, Chen R and Wang Y 2017 *Chem. Phys. Lett.* **686** 103
[28] Die D, Zheng B X, Yue J Y, Guo J J and Du Q 2020 *Physica E* **117** 113805
[29] Fu Y C, Die D, Chen L, Zhu B and Yin H L 2020 *Mol. Phys.* **118** 1622051
[30] Cyrot-Lackmann F and Ducastelle F 1971 *Phys. Rev. B* **4** 2406
[31] Rosato V, Guillope M and Legrand B 1989 *Philos. Mag. A* **59** 321
[32] Cleri F and Rosato V 1993 *Phys. Rev. B* **48** 22
[33] Garip A K 2019 *Mol. Simul.* **45** 1004
[34] Wales D J and Doye J P K 1997 *J. Phys. Chem. A* **101** 5111
[35] Wales D J and Scheraga A H 1999 *Science* **285** 1368
[36] Perdew J P, Burke K and Ernzerhof M 1996 *Phys. Rev. Lett.* **77** 3865
[37] Giannozzi P, Baroni S, Bonini N, *et al.* 2009 *J. Phys.: Condens. Matter* **21** 395502
[38] Giannozzi P, Andreussi O, Brumme T, *et al.* 2017 *J. Phys.: Condens. Matter* **29** 465901
[39] Garip A K 2018 *Int. J. Mod. Phys. C* **29** 1850084
[40] Du R B, Xu Y Q, Wu X and Liu T 2018 *Struct. Chem.* **30** 637
[41] Ferrando R 2018 *Front. Nanosci.* **12** 189
[42] Ferrando R 2015 *J. Phys.: Condens. Matter* **27** 013003